Eur. Phys. J. D (2017) 71: 187
DOI: 10.1140/epjd/e2017-70609-9

THE EUROPEAN PHYSICAL JOURNAL D

Regular Article

Rayleigh Lidar observed atmospheric temperature characteristics over a western Indian location: intercomparison with satellite observations and models*

Som Sharma[a], Rajesh Vaishnav, Krishna K. Shukla, Shyam Lal, Harish Chandra, and Yashwant B. Acharya

Physical Research Laboratory, 380009 Ahmedabad, India

Received 30 September 2016 / Received in final form 21 February 2017
Published online 11 July 2017 – © EDP Sciences, Società Italiana di Fisica, Springer-Verlag 2017

Abstract. General characteristics of sub-tropical middle atmospheric temperature structure over a high altitude station, Mt. Abu (24.5°N, 72.7°E, altitude ∼1670 m, above mean sea level (amsl)) are presented using about 150 nights observational datasets of Rayleigh Lidar. The monthly mean temperature contour plot shows two distinct maxima in the stratopause region (∼45–55 km), occurring during February-March and September-October, a seasonal dependence similar to that reported for mid- and high-latitudes respectively. Semi-Annual Oscillation (SAO) are stronger at an altitude ∼60 km in the mesospheric temperature in comparison to stratospheric region. A comparison with the satellite (Halogen Occultation Experiment, (HALOE)) data shows qualitative agreement, but quantitatively a significant difference is found between the observation and satellite. The derived temperatures from Lidar observations are warmer ∼2–3 K in the stratospheric region and ∼5–10 K in the mesospheric region than temperatures observed from the satellite. A comparison with the models, COSPAR International Reference Atmosphere (CIRA)-86 and Mass Spectrometer Incoherent Scatter Extended (MSISE)-90, showed differences of ∼3 K in the stratosphere and ∼5–10 K in the mesosphere, with deviations somewhat larger for CIRA-86. In most of the months and in all altitude regions model temperatures were lower than the Lidar observed temperature except in the altitude range of 40–50 km. MSISE-90 Model temperature overestimates as compared to Lidar temperature during December-February in the altitude region of 50–60 km. In the altitude region of 55–70 km both models deviate significantly, with differences exceeding 10–12 K, particularly during equinoctial periods. An average heating rate of ∼2.5 K/month during equinoxes and cooling rate of ∼4 K/month during November-December are found in altitude region of 50–70 km, relatively less heating and cooling rates are found in the altitude range of 30–50 km. The stratospheric temperature derived from the Lidar and columnar ozone observed by the Total Ozone Mapping Spectrometer (TOMS) over Mt. Abu shows good correlation ($r^2 = 0.61$) and indicates the association of ozone with the temperature.

1 Introduction

Atmospheric temperature is an important thermodynamical parameter for the study of various geophysical processes and has crucial imprint of radiative, dynamical and chemical behavior of the atmosphere. A detailed study about the climatology of the middle atmospheric temperature by using the different remote sensing techniques has been done around the globe in past two decades [1–6]. The stratospheric temperature observations were carried out by using Lidar over McMurdo Station, Antarctica and the temperature climatology shows that the high temperature variability with descending trend from the stratopause altitude down to the altitude of 30 km [7].

The Lidar observation of the stratospheric temperature are also compared with the MSIS model over Davis, Antarctica and comparison shows that the uniform temperature anomaly of the stratopause region observed by Lidar during midwinter over the observational site than by the MSIS Model [8]. The temperature observations were carried out over the High Arctic at Eureka by using Lidar and meteorological balloons and found the drastic change in the thermal structure of the stratosphere which associated with the wintertime stratospheric vortex [9]. The observation of vortex core is showing insistently cooler lower stratosphere and warmer upper stratosphere. They have observed the different behaviour in the warm annual vortex core from seasonal change in temperature climatology due to change in insolation as well as planetary wave driven sudden stratospheric warming [9]. The Lidar temperature observation over the polar region and its comparison with ECMWF show an agreement in summer season with each other within few Kelvin and higher

* Contribution to the Topical Issue "Low-Energy Interactions related to Atmospheric and Extreme Conditions", edited by S. Ptasinska, M. Smialek-Telega, A. Milosavljevic and B. Sivaraman.

[a] e-mail: somkumar@prl.res.in

temperature is observed in the winter season below 55 km. It is also concluded that the variability in temperature in the winter and summer are maximum and minimum respectively during both the seasons at the scale of day to day variation in the temperature [10]. Middle atmospheric temperature measurements by using Lidar is also studied by various investigators in the past [11–15]. In addition to the imprint of dynamical and radiative processes of the middle atmosphere temperature plays vital role in the Earth's ozone budget (as temperature plays an important role in the ozone chemistry), which is an important and crucial gas to be monitored in the atmosphere [16–21]. Therefore, by studying temperature, we can unravel various aspects of ozone and its chemistry [22–27]. The circulation of the middle atmospheric system, which is also affected by ambient temperatures, determines the residence lifetime of minor species in the atmosphere and their impacts on the structure of the ozone layer in the stratosphere [28]. Despite many observations and simulation studies (based on the input, mostly from high-and mid-latitudes), in the middle atmosphere, the quantitative information from tropical and sub-tropical latitudes and coupling between various geophysical processes understanding the underlying process associated with subtropical region is an important step and is likely to contribute in improving numerical models [29]. In the past, various Lidar studies were limited to mid- and high-latitude stations but there are limited studies in tropical latitudes and very few from sub-tropical region. There is no systematic long term temperature measurements reported from subtropical latitudes in India. Rayleigh Lidar, located at Mt. Abu (an Indian sub-tropical station) is operational and has collected data for ∼50 nights per year since 1997 [30]. Temperature characteristics observed during 1997 to 2001 are presented and discussed in the present study.

2 Observations and data analysis

Lidar observatory is situated on a hill top named 'Gurushikhar' near to Mt. Abu (24.5° N, 72.7° E, altitude ∼1670 m, amsl) and its location is depicted on a topographic map of India shown in Figure 1. The Lidar was operated at Mt. Abu in Rayleigh mode in every year, for about 5 to 10 nights in each month around new moon except during the monsoon (June-July-August) season. Photon counts integrated for 5/10 min were stored. These data are available for more than total 20 nights for most of the months and about 10 nights in June during 1997–2001. Measurements were not made during monsoon season due to cloudy sky condition. Off-line data processing involves adding the photon counts of 5 range bins to give effective range bins of 480 m each. A five-point linear running mean was applied to further smooth the photon count profile. The background noise was removed at this stage, by estimating the average photon counts above 90 km, which was subtracted from each range bin. Range correction was then applied and the densities were obtained from the range corrected photon count profile. Detailed description of data analysis can be found in [30]. The detailed

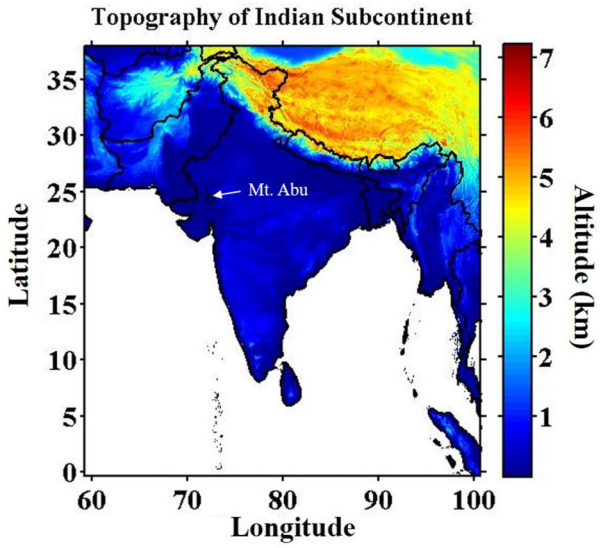

Fig. 1. Location of Mt. Abu is shown on a topographic map of Indian region, showing the orography near to the Lidar observatory.

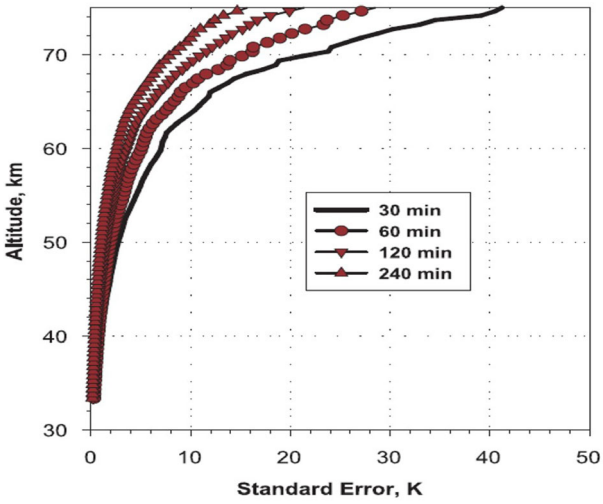

Fig. 2. Effect of temporal integration on error in observed temperatures is shown for 30, 60, 120, and 240 min observations on 21 October 2001 over Mt. Abu.

description about the temperature retrieval methodology used in present study is followed to the previous investigators [31,32].

The continuous observations for 4 h were made during the night of 21 October 2001. Temperature profiles were obtained using different data lengths corresponding to 30, 60, 120 and 240 min. Figure 2 shows the variation of the error with altitude for different data lengths. The error for data length of 30 min varies from about 0.5 K at 40 km to 20 K at 70 km. The errors vary from <0.5 K at 40 km to 15 K at 70 km for 60 min of data length and <0.5 K at 40 km and 11 K at 70 km for 120 and 240 min of data length. In present study, we have used the data which have observation time span longer than 1 h during nighttime.

Usually, observations over the Mt. Abu are carried out for 1–6 h for most of the days.

3 Results

3.1 Observed monthly mean temperature anomalies and seasonal difference in the temperature over Mt. Abu

Mean temperature profiles have been computed from the observed nighttime temperature variation over Mt. Abu. The temperature climatology of the monthly mean (From September to May) data for five years are shown in Figure 3a and similarly, the estimated deviation from the annual mean temperature profile for each month for September to May have been plotted in Figure 3b. We have excluded the days of major Stratospheric Sudden Warming (SSW) in constructing temperature climatology. Every year in the month of September, we have less observation due to extended monsoon period over the observational site. It is clearly seen from the Figure 3a that there is no prominent variation in the temperature at ∼40 km during September to May. Temperature in March is more (∼235 K) as compared to the other months at ∼35 km and also observed the higher temperature in January at ∼40 km with respect to other months. During September-October and March-April in the vernal and autumn equinoxes, we have observed the temperature (∼270 K) pools and it shows that the warming is localized during vernal equinox. Though, autumn equinoctial warming pool is bit extended with maximum during March and another maximum ∼270 K is found during May. The stratopause is the coolest during winter and shows minimum temperature in December.

Mesospheric temperatures show a Semi-Annual Oscillation (SAO) which are very prominently seen at ∼60 km. Maximum and minimum temperature in the height region of 55–70 km, is observed during October/March and in the winter (December–January) respectively. Above 70 km minimum temperatures (∼195 K) were observed during the equinoctial months with a maximum during February (∼220 K). During February-March, higher temperatures are observed at height ∼65–72 km. It is envisaged that higher temperatures are due to frequent occurrence of Mesospheric Temperature Inversions (MTI) during these months. Temperature variability, less than 8–10 K, may not be statistically significant due to the poor signal to noise ratio (SNR) above the ∼70 km. A detailed quantitative scenario of temperature anomalies is given in Table 1 which show the temperature differences from the annual mean temperature. Temperatures are shown at every 5 km in the altitude region from 35 to 70 km during September to May. The maximum (∼+11 K at about 70 km) and minimum temperature (∼–11 K at about 55 km) was found in the month of December and March respectively. Furthermore, from November to December, very strong temperature gradient (∼16 K) is found at altitude of ∼55 km. Similar strong change in temperature is found from February to March at ∼60 km.

We have described the heating and cooling rates of the middle atmosphere from Figure 3b. It is clearly observed in Figure 3b that a prominent cold temperature pool with two eyes type of structure during December and February. A higher temperature during equinoxes and warm temperature pools also observed during both the equinoctial periods (vernal and autumn), exhibit entirely different structure. During vernal equinox, there is strong gradient in the temperature showing upward trend with heating rate of about 2.5 K/month. Inception of warm pool is in the month of October at 45 km and has upward trend and disappears by end of the November (shown in Fig. 3b). In contrast, during autumn there is a downward trend of warm temperature pool in the altitude region of ∼50–60 km. In February, it appears at mesospheric height of ∼72 km and then propagates down to stratosphere (∼45 km) in May. It may propagate further down but could not be tracked during June and July due to local monsoon (Fig. 3a). The rate of cooling during March-April is ∼1 K/month. The highest rate of change of temperature of ∼4 K/month is found in altitude region 50–60 km during October-November and the lowest (<1 K/month) in altitude range of ∼30–40 km. Heating rates are higher, ∼3 K/month in 50–60 km altitude region during September-October and again in February-March. These features have been observed first time in the temperature climatology over a sub-tropical location.

In order to compare the observed Lidar temperature climatology with the HALOE satellite, we have plotted the temperature climatology for the same observation (September-May) period with HALOE in Figure 3c and we also plotted the deviation in the temperature from mean with the HALOE satellite in the Figure 3d. We have taken the HALOE satellite observations at the spatial grid 5° × 5° over Mt. Abu a high altitude site in the western part of India. A significant magnitude difference is observed between the Lidar and the HALOE observed temperatures. The ground-based Lidar as well as HALOE satellite are showing the similar mean stratopause height with a mean temperature difference ∼10 K between both. It is also observed that the spread in the stratopause height is more (height range ∼42–53 km) in Lidar than in the satellite data (height range ∼46–52 km). In the Lidar derived temperature deviations, a strong winter cold temperature pool (about –10 K) is observed in the altitude range of 50–65 km, which is not revealed by satellite observations. A very weak (about –2K) cooling is noted at lower altitudes (35–48 km) during the month of January and February in the satellite observations. The signature of warming during equinoctial months is also found in the Lidar observations but this feature is not delineated in the satellite observations due the coarser grid resolution of the satellite and the observing time difference. A significant temperature difference between Lidar and HALOE observed temperature is found in the various middle atmospheric temperature climatological studies from low and mid latitude stations [2].

We have plotted the monthly mean variation of temperature by using ground-based (Lidar), space-based (HALOE) and model (MSISE-90 and CIRA-86)

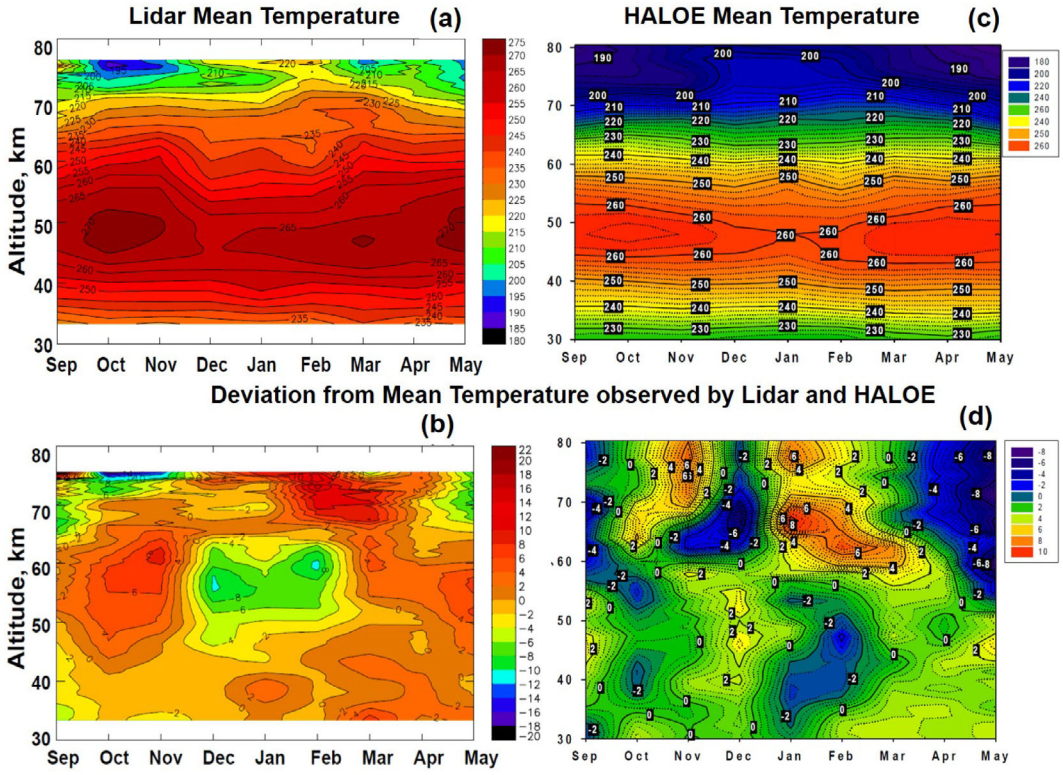

Fig. 3. (a) and (b) Contour plots of monthly mean Lidar observed temperature climatology from 1997–2001 over Mt. Abu is shown in Figure 3a, source: [33]. (b) Similar contour plots for deviations from mean temperature observed by Lidar are shown. (c) and (d) Contour plots of monthly mean HALOE observed temperature climatology from 1997–2001 over Mt. Abu is shown in Figure 3c, source: [33]. (d) Similar contour plots for deviations from mean temperature observed by HALOE are shown.

Table 1. Monthly temperature deviations (in K) from mean temperature over Mt. Abu (table source [34]).

Height (km)	Sept.	Oct.	Nov.	Dec.	Jan.	Feb.	Mar.	Apr.	May
35	–5.2	–1.3	–1.3	–1.5	1.1	–0.6	4.2	2.2	2.4
40	–2.9	–0.2	–0.8	–1.5	2.5	–0.3	1.7	2.5	–1
45	–2.7	3.1	0.1	–3.2	–1.7	0.3	1.7	–0.3	2.7
50	–0.6	5.4	3.9	–4.9	–3.8	–3.9	–0.7	–0.1	4.8
55	0.8	6.2	6.2	–10.3	–7.5	–7	2.3	2.8	6.2
60	–0.5	4.8	8.9	–7.1	–4.3	–10.6	5	1.7	2.1
65	–6.7	2.1	5.1	0.4	–0.1	–1.9	3.3	–0.9	–1.2
70	–8.9	0.9	1.3	–1.7	–2.1	10.8	11.2	–2.5	–9.1

observation in the different height region from stratosphere to mesosphere. We have taken four height region (a) 30–40 km, (b) 40–50 km, (c) 50–60 km, (d) 60–70 km to have a better understanding about the temperature climatology in stratosphere to mesosphere which is shown in Figures 4a–4d. The observed temperature by Lidar in the altitude region ∼30–40 km shows the variation in temperature between ∼240 and 248 K. A signature of SAO is found, with higher temperatures in October and March. Interestingly, in this altitude region, higher temperature (∼248 K) is observed in January. HALOE temperatures are showing weak variability (∼238–243 K). Contrary to Lidar observations, HALOE observed minimum temperature in January. CIRA-86 and MSISE-90 model temperatures also do not show significant variations. Furthermore, Lidar temperatures are anti-correlated to HALOE and model temperatures in January. Due to presence of stratopause altitude, the altitude range of 40–50 km has its own importance. Lidar temperatures vary between ∼263 and 269 K in this altitude region. A prominent signature of SAO with equinoctial maxima is found and weak cooling is observed during winter months. Nonetheless, HALOE temperatures revealed similar seasonal variation; Lidar temperatures are higher (∼8 K) than HALOE temperatures. Despite, qualitative agreement between CIRA-86, MSISE-90 model and Lidar temperatures; Lidar temperatures in October are higher (∼5 K) than the model temperatures.

Lidar temperatures show very high variability (∼247–264 K) in this altitude region 50–60 km. Besides, strong signature of SAO with maximum temperatures in equinoxes, vernal equinox (September-October) shows

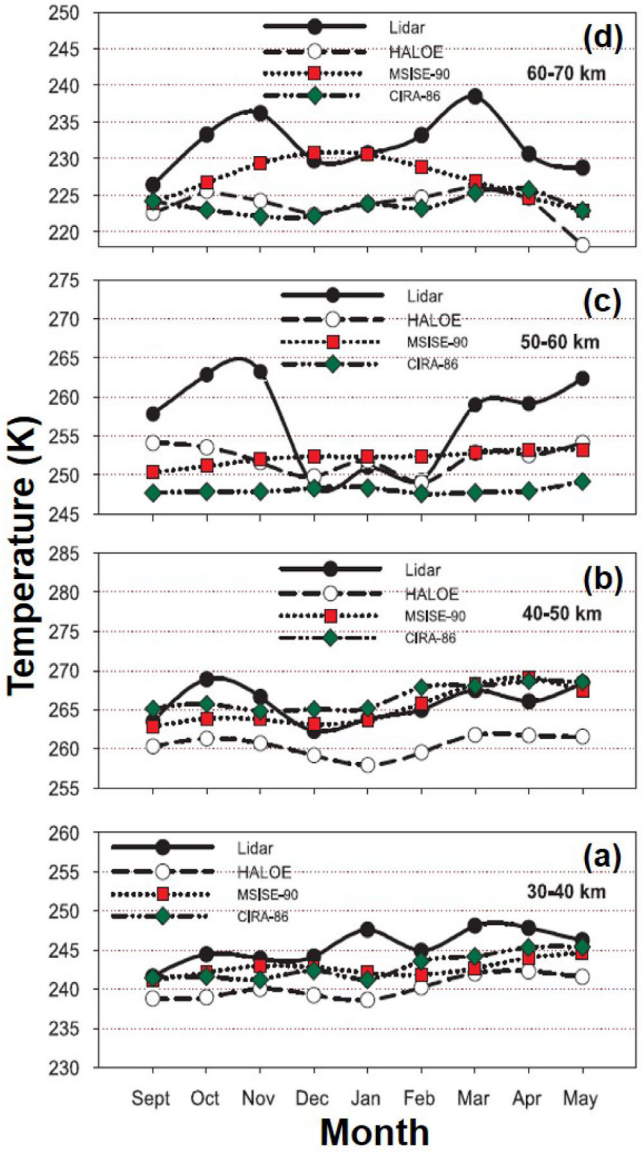

Fig. 4. Monthly mean temperature variation observed by ground-based (Lidar), satellite (HALOE) and models (MSISE-90 and CIRA-86) in the altitude range of (a) 30–40 km, (b) 40–50 km, (c) 50–60 km and (d) 60–70 km over Mt. Abu respectively.

higher temperature than autumn equinox (March-April). Very strong cooling is found during winter months. HALOE temperatures also show a weak SAO. Quantitatively, there are significant differences between Lidar and HALOE temperatures. However, CIRA-86 and MSISE-90 temperature do not show prominent seasonal variations; they differ significantly from each other. CIRA-86 temperatures are about 5 K cooler than that of MSISE-90 temperatures.

In this altitude region ∼60–70 km, Lidar observed temperatures exhibit very strong seasonal variation (∼226–239 K). A clear and strong signature of SAO is present with equinoctial maxima. In contrast to the temperature variation in 50–60 km, autumn maximum is at higher temperature than vernal maximum. However, strong winter cooling is observed from Lidar but weaker than that of 50–60 km altitude region. HALOE temperatures also reveal signatures of SAO but overall monthly mean temperature are significantly cooler (∼12 K) than that of Lidar temperatures. Furthermore, prominent temperature differences (up to ∼8 K) are found between CIRA-86 and MSISE-90 model temperatures. MSISE-90 shows annual oscillation with maximum during winter; which is not revealed by CIRA-86.

Seasonally averaged vertical profile data for winter (December-February) and summer (April-June) are used to study temperatures differences for local winter and summer months over Mt. Abu. We have plotted the vertical profile of seasonal (between winter and summer) difference temperature for Lidar (represented by solid red line), HALOE (represented by dotted blue line), CIRA-86 (represented by dotted green line) and MSISE-90 (represented by dotted magenta line) in Figure 5. The Red and blue arrows are indicating the observed cooler temperatures from Lidar and satellite in Figure 5, respectively. Lidar observations revealed very strong cooling during winter, with a maximum of ∼13 K at an altitude of about 55 km over Mt. Abu. HALOE observations also revealed a cooling (∼8 K) during winter. Lidar observed cooling is about 1.5 times stronger than that of HALOE. Moreover, the height of the Lidar observed coolest region is ∼4 km higher than the HALOE observed coolest region over Mt. Abu. It is to be noted that the errors in the derived temperature are very small (∼1–2 K) in this altitude region. Winter and summer is very significant. Although, studies over mid-latitudes [35] reported winter time cooling but the magnitude of cooling over the Mt. Abu is higher than that of mid-latitude.

Significant difference in winter and summer thermal structures are also observed from Lidar as compared to HALOE and Models in the lower height region (35–45 km). Nevertheless, temperatures differences from Lidar are very small at 40 km, HALOE and Models revealed cooling of about 5 K. In the upper mesosphere also Lidar, HALOE and models revealed higher temperature during winter. HALOE and models are showing very strong warm winter than Lidar observed winter over Mt. Abu.

3.2 Stratospheric temperature and its association with Ozone

Seasonal variation of ozone over a sub-tropical location Mauna Loa [36] also showed lower ozone concentration during winter months. Middle atmospheric ozone and waves have profound effect on the thermal structure and vice versa. During winter months' planetary wave activity is strong and while propagating from lower to middle atmosphere, it modulates atmospheric temperature structure [37,38]. Therefore, we have plotted the monthly mean columnar ozone density over Mt. Abu during 1997–2001 in Figure 6a and also plotted the scatter plot of the stratospheric temperature and ozone to see their association with each other in Figure 6b. We have observed a good

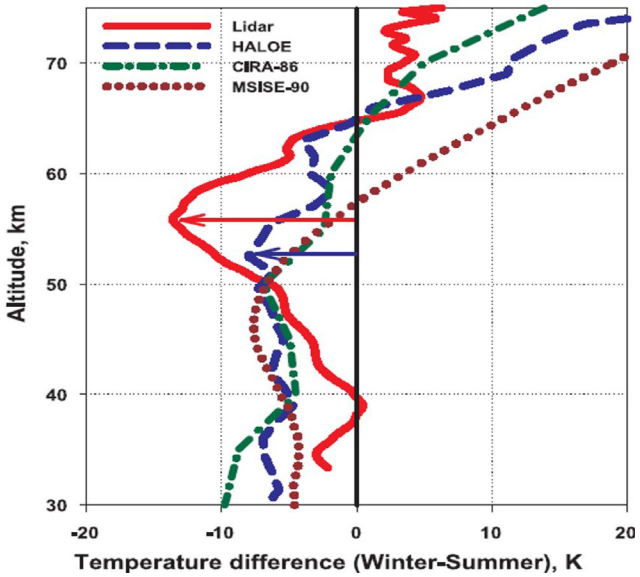

Fig. 5. Winter and summer time temperature differences observed from Lidar and HALOE on board UARS over Mt. Abu. The red and blue arrows are indicating observed cooler temperatures during winter from Lidar and satellite, respectively. Temperature differences during winter and summer for CIRA-86 and MSISE-90 model are also shown in figure.

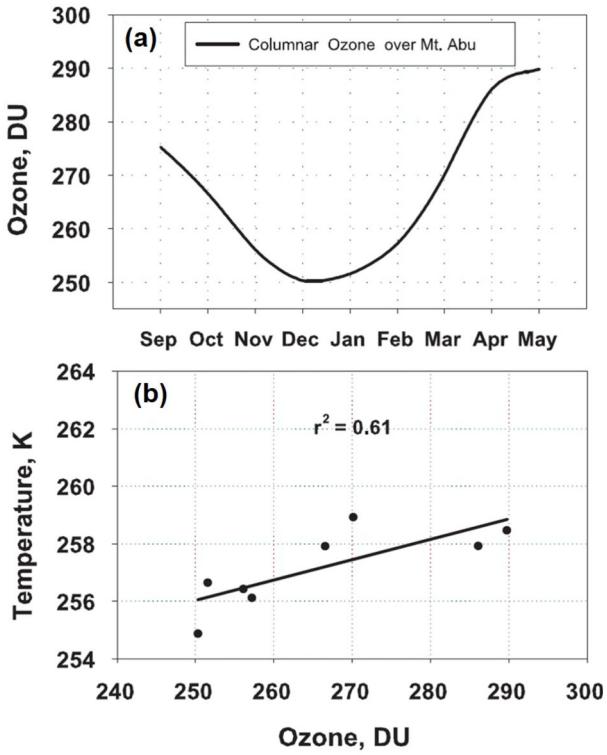

Fig. 6. (a). Monthly mean columnar ozone density in Dobson units (DU) from Total Ozone Mapping Spectrometer (TOMS) over Mt. Abu. (b) Correlation between stratospheric temperature (∼32–46 km) and ozone during 1997–2001.

correlation between temperature and ozone ($r^2 = 0.61$) in Figure 6b which is further strengthens the fact that ozone plays a very vital role in stratospheric thermal structure over a sub-tropical location [37,39]. Temperature affects ozone concentration, as in its formation and/or loss, many reactions rates are temperature sensitive. Therefore, ozone and temperature are highly interlinked in the middle atmosphere. Recently, association of the stratospheric thermal structure with the ozone distribution using chemistry-climate model (CCM) is also explored [40]. They validated ozone and temperature fields using estimates based on observations. Their ozone-change experiments revealed that the thermal structures of the general circulation model (GCM) and CCM respond in a similar manner to ozone differences between 1980 and 2000. Ozone variability is more sensitive to changes in the temperature and vice versa in the tropical and subtropical regions; possibly due to its lower concentrations (∼250 DU) in these regions.

Stratosphere and mesosphere have an entirely different thermal structure (positive/negative temperature gradient). Therefore, associated geophysical processes in these regions are also different. Stratosphere is very stratified and less turbulent due to its stable thermal structure and mesosphere is turbulent due to negative temperature gradient. Stratospheric processes are strongly coupled with the stratospheric ozone due to maximum ozone in this region (at ∼27 km). In order to comprehend stratospheric processes, the study of ozone, its association with temperature, and their interdependence, is indispensable [41,42]. Stratospheric thermal structure has strong imprint of ozone and it is possibly steered by the heating caused by UV absorption by the stratospheric ozone [41,42].

4 Discussion

Middle atmospheric temperature climatology gives new insights in the middle atmospheric characteristics as highlighted previously. An annual and semiannual cycle is dominant at mid-latitudes and lower latitudes respectively. In the present study, we found signature of quasi annual cycle with minimum temperature during winter and higher temperature during equinoxes. The observed downward propagating temperature trend in the mesosphere points out the dominant wave driven pattern, in contrast with the vertically stationary behavior observed below 45–50 km. Similar finding has been reported from the Lidar observations at Mauna Loa another sub-tropical, high altitude station in the northern hemisphere. Maximum variability in the mesosphere is observed in winter over Mt. Abu which is due to (a) maximum planetary wave activity in winter and (b) due to the occurrence of the MTI.

The systematic deviation in the Rayleigh Lidar temperature climatologies were observed in comparison to the CIRA-86 and MSISE-90 models over Mt. Abu, which are similar (cooler stratopause regions in the winters) to the previous comparisons at mid-latitude [43,44]. In particular, cold temperatures in the CIRA-86 model lead to a large difference of more than 12 K around 70-75 km compared to Lidar results. This could be due to an overestimation of non-local thermodynamic equilibrium effects

in the computation of the CIRA-86 temperatures and MTI. On an annual basis CIRA-86 temperatures seem to be too warm around 55–60 km and too cold between 60 and 75 km. Using too cold CIRA-86 temperatures at 80–90 km for initialization can lead to temperature errors at the very top of the Rayleigh Lidar profiles. In this context the model needs to be improved by using more observational input from sub-tropical locations.

It is more likely that the observed departure in the middle and upper mesosphere is related to tidal effects and/or the mesopause thermal SAO over Mauna Loa. The amplitudes of 1–5 K were predicted by tidal models [45]. The climatology presented in this paper was obtained using composite temperature profiles from five years of measurements. Non negligible interannual variability may disturb the temperature field from year to year. However, the features observed in previous climatologies [43,46] remain small compared to the seasonal variations observed over Mt. Abu. Stratospheric cooling and warming are associated with the concentration of ozone and CO_2 [47,48]. Reasonably good correlation ($r^2 = 0.61$) is found in the observed stratospheric temperature and total column ozone over Mt. Abu which shows an admixture of tropical and mid-latitude processes and also the association of ozone production/loss with the temperature over the observational site. It is also reported that there is circumstantial evidence that the stratospheric temperature oscillations (heating or cooling) could be driven by the meridional winds, which in turn could be generated by wave generation and interaction [49] and concluded with a statement, "more definite conclusion, however, must await simultaneous coordinated temperature and wind measurement at common altitudes". However, it is worth noticing that two maxima appearing in the 54–65 km during April-May and September-November over Mt. Abu are in corroboration with the secondary maximum in gravity wave activity observed in the mid-latitudes [50]. Part of the variability of monthly averages and climatology over Mt. Abu can be explained by mesoscale fluctuations with temporal and spatial scales long enough and not filtered out on single observation session during a night. Gravity waves are primarily responsible for these short-scale and short-term fluctuations [51]. As nightly mean profiles are used in this study, therefore it is rather not possible to explain role of gravity waves in the shorter period fluctuations. This is mainly due to natural day to day variability of gravity wave activity induced by changes in low level forcing and mean winds [50].

Observations over Mt. Abu revealed that the average height of stratopause is ∼48 km which is in agreement with observed mean height of stratopause at Gadanki [2] and with rocket measurements from Trivandrum [15]. The spread in stratopause height is about 9 km over Mt. Abu and the spread has a maximum of about 12 km in winter and ∼6 km in summer. Observed stratopause temperatures over Mt. Abu are higher than those are at Gadanki [52]. This is attributed to enhanced orographically generated waves. These waves have significant contribution in causing double stratopause and in modulating temperatures structure. Present study clearly brought out that there is significant difference in the Lidar and satellite observed temperatures in the middle atmosphere. Comparison with empirical models (CIRA-86 and MSISE-90) also revealed prominent difference between Lidar observed and model temperatures. The retrieval methodology of temperature is different for Lidar and models and to a certain extent this can contribute in the observed difference between observations and model. The spatial and temporal geophysical effects could also be played an important role in the observed discrepancies in the temperature over the site.

5 Summary and conclusions

Temperature climatology has been established in the altitude region of 30–75 km using Rayleigh Lidar data over Gurushikhar, Mt. Abu a sub-tropical high altitude site in the western India. A significant month to month difference is observed in the temperature climatology over the observational site. The stratopause altitude varies between 44 and 52 km with a mean value of ∼48 km and also stratopause temperature varies between 260 and 280 K with a mean value of 271 K. Both the stratopause height and temperature are lowest during winter months. Winter is about 12 K cooler than the summer in the height range ∼45–65 km. A cold winter pool is found in altitude region of about 45–60 km and in both the equinoxes warm temperature pool with upward and downward propagating tendencies is also observed. Good correlation between total column ozone and stratospheric temperature is found over Mt. Abu which implies that the temperature plays an important role in the production/loss of the stratospheric ozone. This is first observational evidence from sub-tropical region that the temperature climatology over Mt. Abu is closer to the climatological features of mid-latitude rather than low latitude. Most important finding of the present study is the detection of profound cooling in the upper stratosphere and lower mesosphere during winter over Mt. Abu. Satellite observations and models predictions have not revealed such a strong cooling. It is envisaged that the observed cooling could affect the middle atmospheric chemistry; as many of the rate constants are temperature dependent and scenario of ozone recovery and/or loss may also be affected in these regions. Besides climatological aspects of temperature, present study is also significant in view of increasing thrust on stratospheric-tropospheric coupling and its possible implication on the tropospheric ozone budget, which is modulated by the stratospheric ozone intrusions [53,54]. The use of such a complete climatology is important for many purposes such as providing a reference atmosphere for models, validation of satellite based instruments, and overall comprehension of the strongly coupled lower-middle-upper atmosphere, etc. With the recent and future development of ground-based Lidar network in India, a comprehensive climatology of the middle atmospheric temperature in the low and sub-tropical latitude

ought to be available in the coming years and will be extremely useful in improving models predictability.

Authors are thankful to the team members of the Upper Atmosphere Research Satellite (UARS) Project and the Distributed Active Archive Center at the Goddard Space Flight Center, Greenbelt, Maryland, for providing HALOE satellite data. Team members of Total Ozone Mapping Spectrometer (TOMS) are acknowledged. This work is supported by Department of Space, Government of India.

Author contribution statement

S.S. took observation and analysed Mt. Abu data and wrote paper. R.V. and K.K.S. help in making few figures and in writing of the paper. H.C., S.L. and Y.B.A. help in writing the paper and in discussions. H.C. and Y.B.A. helped in observations and in up keeping lidar at Mt. Abu.

References

1. J.B. Nee, S. Thulasiramana, W.N. Chen, M.V. Ratnam, D.N. Rao, J. Atmos. Sol. Terr. Phys. **64**, 1311 (2002)
2. V. Sivakumar, P.B. Rao, M. Krishnaiah, J. Geophys. Res. **108**, 4342 (2003)
3. C.Y. She et al., Res. Lett. **30**, 1319 (2003)
4. W.J. Randel et al., J. Clim. **17**, 986 (2004)
5. P.S. Argall, R.J. Sica, Ann. Geophys. **25**, 27 (2007)
6. T. Li, T. Leblanc, I.S. McDermid, J. Geophys. Res. **113**, D14109 (2008)
7. G.D. Donfrancesco, A. Adriani, G.P. Gobbi, F. Congeduti, J. Atmos. Terr. Phys. **58**, 1391 (1996)
8. A.R. Klckouciuk, M.M. Lambert, R.A. Vincent, Adv. Space Res. **32**, 771 (2003)
9. T.J. Duck, J.A. Whiteway, A.I. Carswell, J. Geophys. Res. **105**, 909 (2000)
10. A. Schöch, G. Baumgarten, J. Fiedler, Ann. Geophys. **26**, 1681 (2008)
11. M.N. Sasi, K. Sengupta, A model equatorial atmosphere over the Indian zone from 0 to 80 km, Scientific report, ISRO–VSSC–SR–19, 1979
12. S. Lal, B.H. Subbaraya, V. Narayanan, Space Res. **19**, 147 (1979)
13. B.H. Subbaraya, S. Lal, Pure Appl. Geophys. **118**, 581 (1980)
14. M.N. Sasi, Ind. J. Rad. Space Phys. **23**, 299 (1994)
15. K. Mohankumar, Ann. Geophys. **12**, 448 (1994)
16. S. Lal, Studies in equatorial neutral atmosphere, Ph.D. thesis, Gujarat University, 1981
17. B.H. Subbaraya, S. Lal, Proc. Indian Acad. Sci. (Earth Planet. Sci.) **90**, 173 (1981)
18. M. Naja, S. Lal, Geophys. Res. Lett. **23**, 81 (1996)
19. T. Leblanc, I.S. McDermid, J. Geophys. Res. **106**, 14,869 (2001)
20. L.K. Sahu, S. Lal, Geophys. Res. Lett. **33**, L10807 (2006)
21. V. Eyring et al., J. Geophys. Res. **12**, D16303 (2007)
22. J.P.F. Fortuin, H. Kelder, J. Geophys. Res. **103**, 31,709 (1998)
23. H.A. Michelson, G.L. Manney, M.R. Gunson, R. Zander, J. Geophys. Res. **103**, 28, 347–28, 359 (1998)
24. T.G. Shepherd, Chem. Rev. **103**, 4509 (2003)
25. W. Steinbrecht, B. Hassler, H. Claude, P. Winkler, R.S. Stolarski, Atmos. Chem. Phys. **3**, 1421 (2003)
26. S.H.E. Hare, L.J. Gray, W.A. Lahoz, A.O. Neill, L. Steenman-Clark, J. Geophys. Res. **109**, D05111 (2004)
27. P. Keckhut et al., J. Environ. Monit. **6**, 721 (2004)
28. D.J. Karoly, Science **302**, 236 (2003)
29. W.J. Randel et al., J. Clim. **17**, 986 (2004)
30. H. Chandra, S. Sharma, Y.B. Acharya, A. Jayaraman, J. Ind. Geophys. Union **9**, 279 (2005)
31. A. Hauchecorne, M.L. Chanin, Geophys. Res. Lett. **7**, 565 (1980)
32. M.L. Chanin, J. Geophys. Res. **10**, 9715 (1981)
33. T. Leblanc, I.S. McDermid, J. Geophys. Res. **105**, 14,613 (2000)
34. T. Leblanc, I. Mcdermid, A. Hauchecorne, P. Keckhut, J. Geophys. Res. **107**, 6177 (1998a)
35. T.G. Shepherd, J. Met. Soc. Jpn B **85**, 165 (2007)
36. T. Leblanc, A. Hauchecorne, J. Geophys. Res. **102**, 19,471 (1997)
37. P. Keckhut et al., J. Geophys. Res. **101**, 10,299 (1996)
38. D. Pancheva et al., J. Geophys. Res. **113**, D12105 (2008)
39. L.L. Hood, R. McPeters, J. McCormack, L. Flynn, S. Hollandsworth, J. Gleason, Geophys. Res. Lett. **20**, 2667 (1993)
40. P.H. Wang, M.P. McCormick, W.P. Chu, J. Lenoble, R.M. Nagatani, M. L. Chanin, R.A. Barnes, F. Schmidlin, M. Rowland, J. Geophys. Res. **97**, 843 (1992)
41. R.T. Clancy, D.W. Rusch, M.T. Callan, J. Geophys. Res. **99**, 19,001 (1994)
42. M.E. Hagan, J.M. Forbes, F. Vial, On modelling migrating solar tides, Geophys. Res. Lett. **22**, 893 (1995)
43. F.T. Huang, H.G. Mayr, C.A. Reber, Ann. Geophys. **23**, 1131 (2005)
44. G. Gobbi, Ann. Geophys. **13**, 648 (1995)
45. R.A. Wilson, A. Hauchecorne, M. Chanin, Geophys. Res. Lett. **17**, 1585 (1990)
46. S. Sharma, V. Sivakumar, H. Chandra, P.B. Rao, Adv. Space Res. **7**, 2278 (2006)
47. W.K. Hocking, T. Carey-Smith, D.W. Tarasick, P.S. Argall, K. Strong, Y. Rochon, I. Zawadzki, P.A. Taylor, Science **450**, 281 (2007)
48. S.S. Das, Geophys. Res. Lett. **36**, L15821 (2009)
49. W. Chen, H.-F. Graf, M. Takahashi, Geophys. Res. Lett. **29**, 2073 (2002)
50. W. Chen, T. Li, J. Geophys. Res. **112**, D20120 (2007)
51. G. Branstator, J. Atmos. Sci. **41**, 2163 (1984)
52. M. Ting, M.P. Hoerling, T. Xu, A. Kumar, J. Clim. **9**, 2615 (1996)
53. S. Sharma, Lidar studies of middle atmospheric density and temperature structures over Mt. Abu, Ph.D. thesis, Gujarat University, Ahmedabad, India, 2010
54. S. Sharma, S. Sridharan, H. Chandra, S. Lal, Y.B. Acharya, Planet. Space Sci. **63**, 36 (2012)
55. S. Pawson, R.S. Stolarski, A.R. Douglass, P.A. Newman, J.E. Nielsen, S.M. Frith, M.L. Gupta, J. Geophys. Res. **113**, D12103 (2008)
56. A. Robock, Science **272**, 972 (1996)
57. C. Cagnazzo, C. Claud, S. Hare, Clim. Dyn. **27**, 101 (2006)
58. A. Hauchecorne, M. Chanin, P. Keckhut, J. Geophys. Res. **15**, 297 (1991)
59. V. Ramaswamy et al., Rev. Geophys. **39**, 71 (2001)